Atomistic Simulations of Oleic Imidazolines Bound to Ferric Clusters

Sunder Ramachandran,[†,‡] Bao-Liang Tsai,[†] Mario Blanco,[†] Huey Chen,[§] Yongchun Tang,[§] and William A. Goddard III*[,†]

Materials and Process Simulation Center, Beckman Institute (139-74), Division of Chemistry and Chemical Engineering, California Institute of Technology, Pasadena, California 91125, and Chevron Petroleum Technology Company, 1300 Beach Boulevard, La Habra, California 90631

Received: July 10, 1996; In Final Form: October 11, 1996[⊗]

The oleic imidazoline (OI) class of molecules is used extensively for corrosion inhibitor oil field pipeline applications. However, there is no model for understanding how they work. As a first step in elucidating this mechanism we carried out quantum mechanical calculations on clusters involving Fe^{3+}, H_2O, OH, and OI. These calculations are used to determine the MS force field for molecular dynamics simulations.

1.0 Introduction

Corrosion causes enormous industrial expense leading to a large market for corrosion inhibitors. Development of such corrosion inhibitors has been slowed because *the mechanism by which these chemical compounds prevent corrosion is not understood*.[1] Experimental evidence in support of specific mechanisms is difficult because

i. they are used in low concentrations (a few parts per million),

ii. the operating environments are quite complex, and

iii. it is difficult to experimentally observe the atomistic nature of the fluid/metal interface.

In this paper we report quantum chemical (QC) calculations on clusters involving oleic imidazoline (OI) inhibitors and develop the MS force field (FF) to be used in molecular dynamics (MD) simulations. As a model OI, we use the molecule 1,2-dimethylimidazoline (OI-1-C) in Figure 1.

2.0 Results

2.1 The GVB Model of Fe_2O_3. At pH values in the range of 4−6 (for oil field applications the pH ∼ 4.5), the stable oxide[2,3] of Fe is α-Fe_2O_3 (hematite). Thus we expect that the Fe surface will be covered by this native oxide. Consequently we studied the interactions of OI with the Fe_2O_3 surface. In α-Fe_2O_3 crystal the Fe is in a distorted octahedral site with three bonds at 1.946 Å (with OFeO bond angles of 111.8°) and three at 2.116 Å.[4] The GVB model of Fe_2O_3 postulates that the bonding in Fe_2O_3 can be described as follows:

1. There are three covalent partially ionic (CPI) bonds with bond distances of 1.946 Å. These correspond to the formal charge of +3. Each CPI bond involves some 4s and 4p atomic character on the Fe as the electron in each orbital is partially transferred to the oxygen atom.

2. The Fe also has five electrons in d orbitals (a d^5 configuration) coupled to high spin ($S = {}^5/_2$).

3. The remaining three Fe···O bonds (2.116 Å) are of donor−acceptor (DA) or Lewis base−Lewis acid type. This involves a lone pair on the O (the Lewis base) coordinating to the Fe (the Lewis acid).

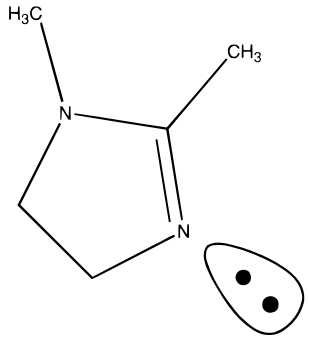

Figure 1. 1,2-Dimethylimidazoline used as a model for OI corrosion inhibitors. (The ring CH_2 groups are implicit.) The lone pair that coordinates to the Fe is indicated.

2.2 Cluster Calculations for Fe_2O_3. To test the GVB model of Fe_2O_3, we first carried out QC calculations[5−8] (RHF/LAV3P*) on the $Fe(OH)_3(H_2O)_3$ cluster. We find the structure in Figure 2 with three CPI bonds of 1.916 Å (with OFeO bond angles of 109.3°) and three DA bonds of 2.259 Å. In the GVB model the CPI bond should be approximately trans to a DA bond, and indeed the cluster leads to an average angle of 160.3° while the crystal leads to 162.2°. Also the Fe−O−Fe bond angle in hematite between CPI bonds is 119.7°, while the Fe−O−H bond angle in the cluster is 121.8°. The close correspondence of the geometries for the $Fe(OH)_3(H_2O)_3$ cluster and the Fe_2O_3 crystal confirms the GVB model of Fe_2O_3.

To examine the character of the orbitals, we carried out GVB calculations. Here we correlated the three Fe−O CPI bonds, the three Fe−OH_2 DA bonds, and all nine OH bonds [GVB-(15/24)]. Figure 3a shows the two Fe···O GVB orbitals for the Fe−OH CPI bond. One orbital corresponds closely to an sp^3 hybrid orbital on the O, while the other has some Fe sp character in addition to the O character. The GVB overlap is 0.87, indicating a fairly ionic bond. The covalent nature of the bond is shown in the buildup of electron density between the atoms. The ionic nature is clear by the large participation of the oxygen orbitals in the both GVB orbitals. Figure 3b shows the two GVB orbitals of a Fe−OH_2 donor−acceptor bond from a GVB calculation correlating all 24 valence pairs (to make the lone pairs unique). Here the orbitals correspond to the lone pair of the oxygen in the H_2O, with in−out or radial correlation. This pair forms a Lewis base to Lewis acid bond to the Fe.

From the QC calculations (RHF/LAV3P*) on the cluster, we developed the MS FF in Tables 1 and 2. [Here the MS denotes that the FF is meant to be used for materials simulations.] This

* To whom correspondence should be addressed.
† California Institute of Technology.
‡ Current Address: Baker Performance Chemicals Incorporated, 3900 Essex Lane, 3rd floor, Houston, Texas 77027.
§ Chevron Petroleum Technology Company.
⊗ Abstract published in *Advance ACS Abstracts,* December 1, 1996.

S1089-5639(96)02041-5 CCC: $14.00

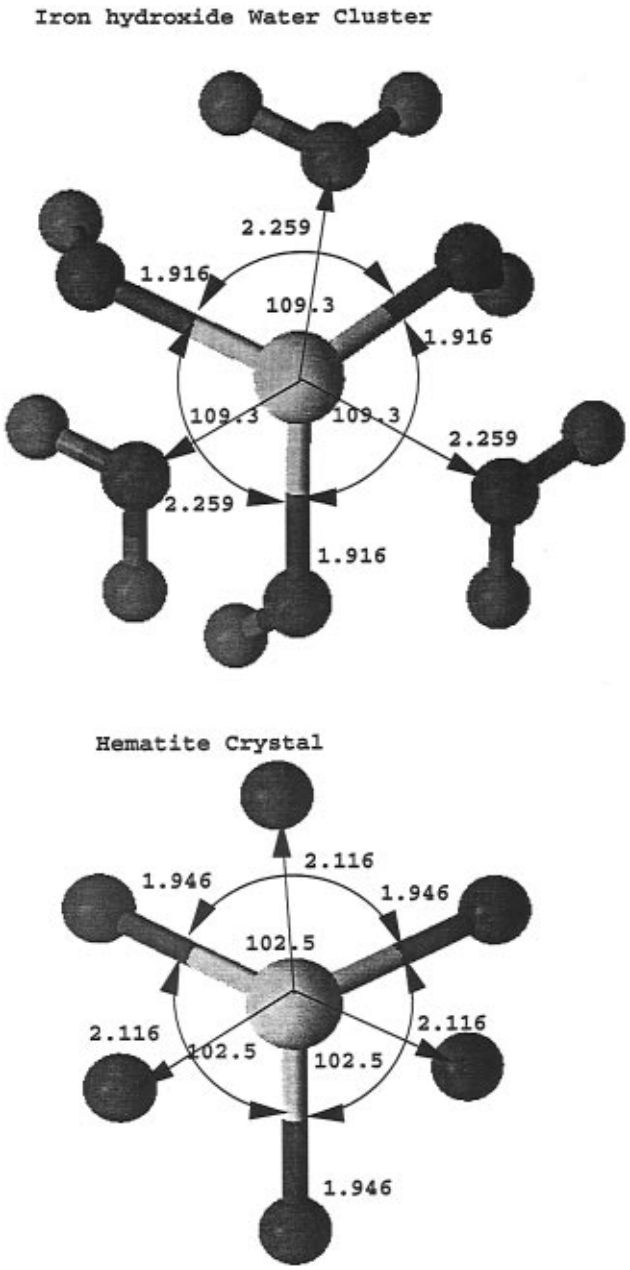

Figure 2. (a) $Fe(OH)_3(H_2O)_3$ cluster optimized using QM (HF/LAV3P*). (b) Geometry from the α-Fe_2O_3 crystal.

FF is based on the generalized valence bond (GVB) model of Fe_2O_3. Thus we distinguish an Fe−OH CPI bond (which uses the Fe-O_3 valence parameters in Table 1A) from the Fe···-OH2 DA bond (which uses the Fe···O_3 nonbond parameters in Table 2B). We started with the Dreiding FF and modified only geometric parameters to fit the QC results. As a test of the GVB model for Fe_2O_3, we then used the MS FF to describe the α-Fe_2O_3 crystal. This leads to lattice parameters of $a = b = 5.00$ Å, $c = 13.76$ Å, which compares well with the experimental lattice parameters $a = b = 5.038$ Å, $c = 13.77$ Å.[4]

2.3 Binding Energies of $Fe(OH)_3(H_2O)_2$ and N-Containing Molecules. We assume that the binding of OI corrosion inhibitor molecules to the iron oxide surface involves Fe−N interactions. In order to model this interaction, we use the GVB model of Fe_2O_3 which suggests that in water the surface Fe can be modeled as $Fe(OH)_3(H_2O)_3$. Thus we used the $Fe(OH)_3(H_2O)_2$(Nmol) cluster to represent OI bond to oxide surface. In order to understand whether OI is special, we calculated the bond energies between various small N-containing molecules (Nmol) and the iron oxide cluster.

We first investigated the GVB model using three different basis set schemes:

i. LANL1DZ—Hay and Wadt's basis (3s2p5d/2s2p2d) and 18-electron effective core potential for Fe,[9] D95V (DZ)[10] basis for the nonmetals.

ii. LAV3P*—Hay and Wadt's basis (3s2p5d/3s2p2d) and 18-electron effective core potential for Fe, 6-31G* basis for the nonmetals.

iii. LACV3P*—Hay and Wadt's basis (9s5p5d/3s3p2d) and 10-electron effective core potential for Fe,[9] 6-31G* basis for the nonmetals.

All calculations with LANL1DZ and LACV3P* were done at the UHF level using the Gaussian 92 program, while with LAV3P* the calculations were done at the RHF level using PSGVB program. Table 3 lists the $Fe(OH)_3(H_2O)_2-H_2O$ bond energy calculated using the three schemes. The LACV3P* basis is the most accurate (including an explicit treatment of the 3s,-3p core electrons); however, Table 3 shows that LAV3P* leads to bond energies within 1 kcal/mol. Thus the simple treatment of only the eight valance electrons on the Fe is adequate. Similarly the smaller LANL1DZ basis gives results comparable to the more extensive LAV3P* basis. Therefore, we used LANL1DZ for all further calculations.

The bond energies calculated (UHF/LANL1DZ) for various N-containing molecules are also listed in Table 3. The snap bond energy shows the electronic effects. Thus NH_3 with $D = 28.8$ kcal/mol is a stronger Lewis base than H_2O with $D = 24.9$ kcal/mol. However, the adiabatic bond energies for NH_3 and H_2O are closer, 12.2 and 11.7 kcal/mol, respectively, indicating the importance of steric effects. These calculations show that the sp^2 ligand $NH{=}CH_2$ bonds to $Fe(OH)_3(H_2O)_2$ comparably with the sp^3 ligand NH_2-CH_3, but both are much better than the sp^1 ligand NCH. We find that the sp^2 ligand imidazoline makes a much stronger bond (41.8 kcal/mol snap bond energy) to the Fe atom of $Fe(OH)_3(H_2O)_2$ than $NH{=}CH_2$, indicating a special role for the imidazoline ring. This extra bonding is consistent with the excellent corrosion inhibition for these OI compounds.

2.4 Binding of OI. On the surface of Fe_2O_3 we expect the OI to bond strongly as a Lewis base to the Fe^{3+}. In aqueous environments we assume that there is an H_2O at this surface site of Fe_2O_3 that must be displaced. Thus we optimized the structure of $Fe(OH)_3(H_2O)_2$ (OI-1-C) with the results in Figure 4. The average Fe−OH distance is 1.930 Å (an increase of 0.014 Å) with an OFeO angle of 106.0° (a decrease of 3.3°). The average DA bond is 2.358 Å to H_2O (an increase of 0.10 Å) with an Fe···OI bond of 2.245 Å.

The snap bond energy (no change in other ligands) is 37.0 kcal/mol for OI compared to 22.3 kcal/mol for H_2O. This indicates that the dative bond due to the Nsp^2 lone pair orbital of OI is considerably stronger than that of the Osp^3 lone pair orbital of H_2O.

Allowing the ligands to relax after breaking the bond (the adiabatic bond energy), the desorption energy for OI is 16.6 kcal/mol versus 12.9 for H_2O. The decreased adiabatic bond energy versus the snap bond energy reflects crowding in the six-coordinate site.

Combining these quantities, we estimate the energetics in (1)

$$Fe(OH)_3(H_2O)_3 + OI \rightarrow Fe(OH)_3(H_2O)_2(OI) + H_2O \quad (1a)$$

$$\Delta E_1^{AD} = -3.7 \text{ kcal/mol (exothermic)} \quad (1b)$$

$$\Delta E_1^{snap} = -14.7 \text{ kcal/mol} \quad (1c)$$

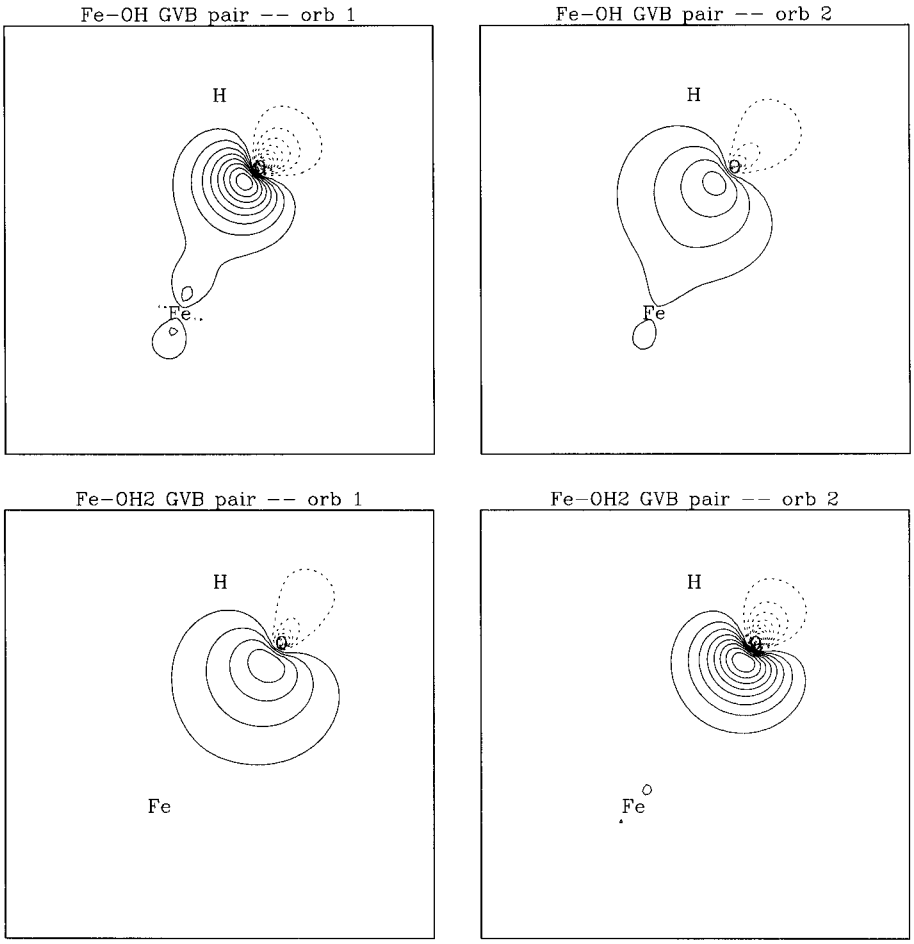

Figure 3. GVB contour diagram of the electron pairs of (a) Fe−OH CPI bond and (b) Fe−OH_2 donor−acceptor bond.

TABLE 1: Valence Parameters for the MS FF[a]

(A) Bond Stretch (Harmonic): $E(R) = {}^1/_2K_b(R - R_b)^2$

type	K_b (kcal/mol/Å)	R_b (Å)	type	K_b (kcal/mol/Å)	R_b (Å)
Fe−O_3	1050.0[a]	1.925[a]	N_3−C_3	700.0[b]	1.462[b]
Fe−O_3z	1050.0[a]	1.972[a]	N_R−C_3	700.0[b]	1.460[b]
O_3−H	700.0[b]	0.98[b]	N_R−C_2	1050.0[b]	1.380[b]
C_2−C_3	700.0[b]	1.430[b]	N_2−C_3	700.0[b]	1.460[b]
C_2−C_2	1400.0[b]	1.330[b]	N_2−C_2	1400.0[b]	1.250[b]
N_3−H	700.0[b]	1.022[b]	C_2−H	700.0[b]	0.9900[b]

(B) Bond Stretch (Morse): $E(R) = D_b[e^{\alpha_b(R-R_b)} - 1]^2$ where $K_b = 2D_b\alpha_b^2$

type	D_b (kcal/mol)	K_b (kcal/mol/Å)	R_b (Å)
C_3−H	95.1[c]	741.372[c]	1.0765[c]
C_3−C_3	85.8[c]	884.994[c]	1.4841[c]

(C) Angle Bend (Harmonic Cosine): $E(\theta) = {}^1/_2C(\cos\theta - \cos\theta_0)^2$ Where $K_\theta = C\sin^2\theta_0$

type	K_θ (kcal/mol)	θ_0 (deg)	type	K_θ (kcal/mol)	θ_0 (deg)
Fe−O_3−X	300.0[a]	124.50[a]	X−N_2−X	100.0[b]	109.47[b]
Fe−O_3z−X	400.0[a]	126.30[a]	X−C_3−X	100.0[b]	109.47[b]
O_3−Fe−O_3	400.0[a]	116.80[a]	X−C_2−X	100.0[b]	120.0[b]
O_3z−Fe−O_3z	300.0[a]	107.60[a]	H−C_3−H	55.6076[c]	119.393[c]
X−N_3−X	100.0[b]	106.70[b]	C_3−C_3−H	65.7301[c]	117.7291[c]
X−N_R−X	100.0[b]	120.00[b]	C_3−C_3−C_3	84.1810[c]	121.24[c]
C_3−N_R−C_2	100.0[b]	109.47[b]			

(D) Torsion: $E(\phi) = {}^1/_2|V_T|(1 - (V_T/|V_T|)\cos P_\phi)$

type	P	V_T[d]	type	P	V_T[d]
X−C_2−C_3−X	3[a]	2.0[a]	C_2−N_2−C_3−X	3[a]	2.0[a]
N_2−C_2−N_R−X	6[a]	−1.0[a]	X−N_2−C_2−X	2[a]	−10.0[a]
O_3−Fe−O_3−X	6[a]	0.5[a]	H−C_3−C_3−H	3[c]	−5.1686[c]
O_3z−Fe−O_3z−X	6[a]	0.5[a]	C_3−C_3−C_3−H	3[c]	−6.1626[c]
X−N_3−C_3−X	3[b]	2.0[b]	C_3−C_3−C_3−C_3[†]	3[c]	−5.7070[c]
X−N_R−C_2−X	2[a]	−2.0[a]			

TABLE 1 (Continued)

(E) Bond−Angle and Bond−Bond Cross-Terms: $E_{ax} = D_1(\cos\theta - \cos\theta_0)(R_1 - R_{b1}) + D_2(\cos\theta - \cos\theta_0)(R_2 - R_{b2}) + K_{rr}(R_1 - R_{b1})(R_2 - R_{b2})$

type	D_1 (kcal/mol)	θ_0 (deg)	R_{b1} Å	D_2 (kcal/mol)	R_{b2} Å	K_{rr} (kcal/mol/Å^2)
H−C_3−H	−22.6583[c]	119.393[c]	1.0765[c]	−22.6583[c]	1.0765[c]	3.1321[c]
C_3−C_3−H	−34.3195[c]	117.7291[c]	1.4841[c]	−25.9234[c]	1.0765[c]	1.3684[c]
C_3−C_3−C_3	−54.0185[c]	121.24[c]	1.4841[c]	−54.0185[c]	1.4841[c]	26.2187[c]

(F) Inversion (Cosine Harmonic) $E(\psi) = {}^1/_2C(\cos\psi - \cos\psi_0)^2$ Where $K_\psi = C\sin^2\psi_0$

type	K_ψ (kcal/mol)	ψ_0 (deg)
C_2−X−X−X	5.00[a]	0.0[b]
N_R−X−X−X	6.80[a]	40.0[a]

[a] Values optimized in this paper. [b] Values from ref 12. [c] Values from ref 13. [d] Positive implies that the cis configuration is maximum, whereas negative implies that it is a minimum.

TABLE 2: van der Waals Parameters for the MS FF[a]

(A) Diagonal Nonbond Terms (exp-6):
$E(R) = D_v\{[6/(\zeta - 6)]\exp[\zeta(1 - r)] - [\zeta/(\zeta - 6)]\rho^{-6}\}$
Where $\rho = R/R_v$

type	R_v (Å)	D_v (kcal/mol)	ζ
H_	3.166 50[c]	0.020 00[c]	11.200 0[c]
O_3	3.404 60[b]	0.095 70[b]	13.483[b]
O_2	3.404 60[b]	0.095 70[b]	13.483[b]
Fe	4.540 00[b]	0.055 00[b]	12.000 0[b]
C_3	3.48 10[c]	0.079 18[c]	13.000 0[c]
C_2	3.841 00[c]	0.079 18[c]	13.000[c]
N_3	3.660 00[b]	0.069 00[b]	13.843[b]
N_R	3.660 00[b]	0.069 00[b]	13.843[b]
N_R	3.660 00[b]	0.069 00[b]	13.843[b]

(B) Off-Diagonal Nonbond Terms (Morse):
$E(R) = D_v[\chi^2 - \chi]$
Where $\chi = \exp[{}^1/_2\zeta(1 - \rho)]$ and $\rho = R/R_v$

type	R_v (Å)	D_v (kcal/mol)	ζ
O_3−Fe	2.4180[a]	5.14[a]	11.0[a]
O_3z−Fe	2.4180[a]	5.14[a]	11.0[a]
N_2−Fe	2.2800[a]	8.1[a]	10.0[a]
N_R−Fe	2.2800[a]	8.1[a]	10.0[a]
N_3−Fe	2.432[a]	7.0[a]	11.0[a]

[a] Values optimized in this paper. [b] Values from ref 12. [c] Values from ref 13.

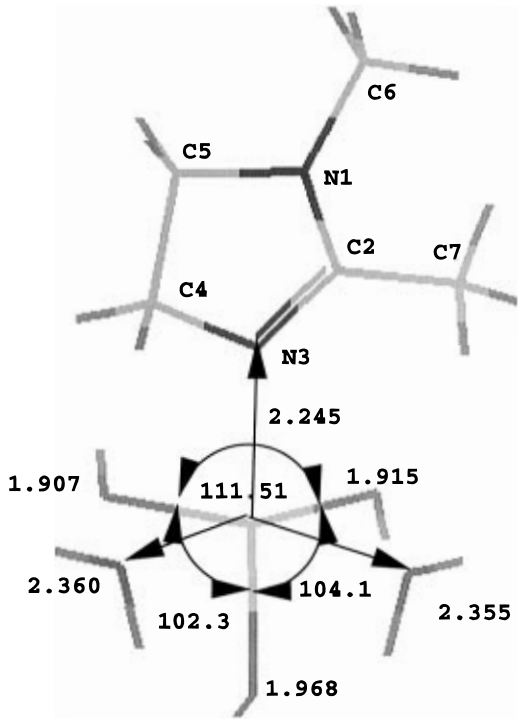

Figure 4. $Fe(OH)_3(H_2O)$ (OI-1-C) cluster optimized using QM (HF/LANLIDZ).

TABLE 3: Bond Energies for $Fe(OH)_3(H_2O)_2$−(molecule) from Quantum Chemical Calculations

	LANL1DZ	LAV3P*	LACV3P*
(a) cluster $Fe(OH)_3(H_2O)_2$−OH_2			
bond energy (Fe···OH_2)			
snap	24.94	22.28	22.46
adiabatic	11.72	12.88	11.75
(b) cluster $Fe(OH)_3(H_2O)_2$−NH_3			
bond energy (Fe···NH_3)			
snap	28.82		
adiabatic	12.24		
(c) cluster $Fe(OH)_3(H_2O)_2$−NH_2CH_3			
bond energy (Fe···NH_2CH_3)			
snap	30.14		
adiabatic	12.28		
(d) cluster $Fe(OH)_3(H_2O)_2$−$NHCH_2$			
bond energy (Fe···$NHCH_2$)			
snap	29.46		
adiabatic	12.49		
(e) cluster $Fe(OH)_3(H_2O)_2$−NCH			
bond energy (Fe···NCH)			
snap	11.85		
adiabatic	0.44		
(f) cluster $Fe(OH)_3(H_2O)_2$−OI			
bond energy (Fe···OI)			
snap	41.77	36.89	
adiabatic	14.76	16.57	

Removing an H_2O from the OI complex leads to (2)

$$Fe(OH)_3(H_2O)_2(OI) \rightarrow Fe(OH)_3(H_2O)(OI) + H_2O \quad (2a)$$

$$\Delta E^{AD} = +9.7 \text{ kcal/mol} \quad (2b)$$

$$\Delta E^{snap} = +20.6 \text{ kcal/mol} \quad (2c)$$

These calculations indicate that OI adsorbs to the iron cluster more strongly than water. On the Fe_2O_3 surface, constraints due to the Fe_2O_3 framework should lead to energetics intermediate between snap (which allows no ligand rearrangement) and adiabatic (allowing full rearrangement). In addition, we expect that the Fe for the Fe_2O_3 surface will be more positive than in the cluster (since neighboring Fe are more electron-positive than H), leading to larger bond energies. This agrees with the experimental observation that OI molecules absorb rapidly.[11]

2.5 The MS FF. *2.5.1 Valence Parameters.* We developed the MS FF to describe the geometries and energetics based on these cluster results. This is based on the GVB model of bonding. Thus we consider that there are three CPI Fe−O bonds using the valence parameter of Table 1 and three DA Fe···O bonds using the nonbond parameters of Table 2.

We started with the Dreiding[12] FF (using the exponential-six vdW parameters) and the MSXX FF for hydrocarbons[13] and modified them based on QC calculations on clusters.

The standard Dreiding atom types are used. Thus O_3 is an sp^3 O used in H_2O. The iron atom in the ferric clusters is

denoted as Fe. The oxygen atom in the hydroxyl groups of the ferric clusters is also denoted as O_3. The QC studies show that the O−Fe−O angle is 109.3° in the ferric cluster but 102.3° in hematite. Thus we define an O_3z atom type to be used in hematite. We use N_R to denote the nitrogen atom in the 1 position in the ring (involved in a π bond), while N_2 denotes the sp^2 nitrogen atom in the 3 position of the imidazoline ring (the atom coordinated to the Fe). The sp^3 nitrogen atom in amino ethyl side groups is denoted as N_3. The sp^3 and sp^2 carbon atoms are denoted as C_3, and C_2 atom types.

Table 1 describes the valence interaction terms of the MS FF. The terms are obtained from the Dreiding FF[12] and MSXX FF for hydrocarbons[13] with adjustments made to reproduce the ferric cluster and imidazoline ring QM results. The bond stretch force constants for iron−oxygen interactions use the Dreiding FF values for bond order of $1^1/_2$. The following valence interactions are used where where

i. harmonic bond stretch terms

$$E(R) = {}^1/_2K_R(R - R_e)^2 \quad (3)$$

ii. Morse bond stretch terms

$$E(R) = D_b[e^{\alpha_b(R-R_b)} - 1]^2 \quad (4)$$

$$k_b = 2D_b\alpha_b{}^2 \quad (5)$$

iii. harmonic cosine angle stretch terms

$$E(\theta) = {}^1/_2C(\cos\theta - \cos\theta_0)^2 \quad (6)$$

$$K_\theta = C\sin^2\theta_0 \quad (7)$$

iv. torsional *n*-fold potentials

$$E(\phi) = {}^1/_2|V_T|\left(1 - \frac{V_T}{|V_T|}\cos P\phi\right) \quad (8)$$

v. bond−angle and bond−bond cross-terms of the form

$$E_{ax} = D_1(\cos\theta - \cos\theta_0)(R_1 - R_{b1}) + D_2(\cos\theta - \cos\theta_0)(R_2 - R_{b2}) + k_{rr}(R_1 - R_{b1})(R_2 - R_{b2}) \quad (9)$$

vi. inversion terms of the form

$$E(\psi) = {}^1/_2C(\cos\psi - \cos\psi_0)^2 \quad (10)$$

where

$$K_\psi = C\sin^2\psi_0 \quad (11)$$

It also has one-center angle−angle cross-terms and two-center angle−angle terms identical to the type given by Karasawa, Dasgupta, and Goddard[13] for the hydrocarbon interactions (pertaining to atom types C_3 and H).

Nonbond interactions are charaterized by electrostatic and van der Waals interactions. The van der Waals interactions have exponential-six and off-diagonal Morse potentials. These are given in Table 2.

TABLE 4: Charges (electron units) for $Fe(OH)_3(H_2O)_3$, Imidazoline, and α-Fe_2O_3

	MS FF	QM
(a) $Fe(OH)_3(H_2O)_3$		
Fe	1.56	1.56
O (OH)	−0.98	−1.04
H (OH)	0.46	0.41
H (H_2O)	0.41	0.43
O (H_2O)	−0.82	−0.75
(b) 1,2-Dimethylimidazoline (See Figure 4)		
N1 (1 position on ring)	−0.240	−0.344
C2 (2 position on ring)	0.800	0.826
N3 (3 position on ring)	−0.560	−0.783
C4 (4 position on ring)	−0.288[a]	0.393
C5 (5 position on ring)	−0.288[a]	−0.261
C6 (1-methyl)	−0.432[a]	−0.311
C7 (2-methyl)	−0.432[a]	−0.604
H8 (C4 Hydrogen)	0.144[a]	−0.016
H9 (C4 Hydrogen)	0.144[a]	−0.009
H10 (C5 Hydrogen)	0.144[a]	0.108
H11 (C5 Hydrogen)	0.144[a]	0.119
H12 (C6 Hydrogen)	0.144[a]	0.161
H13 (C6 Hydrogen)	0.144[a]	0.113
H14 (C6 Hydrogen)	0.144[a]	0.113
H15 (C7 Hydrogen)	0.144[a]	0.159
H16 (C7 Hydrogen)	0.144[a]	0.174
H17 (C7 Hydrogen)	0.144[a]	0.160
(c) α-Fe_2O_3 Crystal		
Fe	1.317	
O	−0.878	

[a] Charges fixed to values from ref 13.

2.5.2 Charges. Potential-derived charges (PDQ) were obtained from QC calculations on Fe clusters and the imidazoline head group. These are shown in Table 4. Adjustments were made to eliminate effects of charge transfer as shown in Table 4. In order to be able to predict charges for various substitutions of the OI and for the Fe_2O_3 surface, we modified the QEq parameters[14] to reproduce the QC charges. These new QEq* parameters are $X_{Fe} = 3.100$ eV, ${}^1/_2J_{Fe} = 3.400$ eV, and $R_{Fe} = 1.30$ Å. These values were then used in the extension of the QEq method[14] for periodic systems[15] to determine charges in hematite (see Table 4). Charges on the hydrocarbon tail are determined identically as for MSXX FF[13] (making each methylene unit electrically neutral, see Table 4). The charges on water were taken from Stillinger and Rahman[16] (see Table 4). The charges for hydroxyl and amine compounds used in a later papers[17] follow the MSXX FF convention (keeping each functional group electrically neutral) with the hydrogen atoms of hydroxyl and amine groups at 0.45 and 0.36, respectively.

2.5.3 Validation. The results from MSX FF calculations on the cluster are compared with QC results in Table 5. The structures and energetics of the adiabatic (minimum energy) structures for the MS FF are in excellent agreement with the QC. The snap bond energy for QC is larger than for the FF. This probably arises from the assumption of constant charges assumed in the FF. We consider it more important that the adiabatic energies be well described.

2.6 The Pendant Group. Most OI CI have a short pendent group, e.g. $-CH_2-CH_2-X$, where X is polar (X = NH_2 or OH). These polar groups can form a DA bond to a second Fe at the surface. Although this would appear to be beneficial, replacement with an alkyl group[1] seems to work nearly as well. Thus OI-17(8═9)-CCN (1-aminoethyl-2-oleicimidazoline) and OI-17(8═9)-C (1-methyl-2-oleicimidazoline) lead to CIE (corrosion inhibition efficiency) of 92% and 90%, respectively. However, replacement of the pendent group with H [OI-17-(8═9)-H](2-oleicimidazoline) leads to a dramatic decrease to CIE = 77%. In order to determine the origin of this effect, we

TABLE 5: Comparison between Quantum Mechanical and FF Results for $Fe(OH)_3(H_2O)_3$ and $Fe(OH)_3(H_2O)_2$ (OI-1-C)

	MS FF	QM (LAV3P*)
(a) Cluster $Fe(OH)_3(H_2O)_3$		
Fe···OH_2	2.259 Å	2.259 Å
Fe−OH	1.916 Å	1.916 Å
HO−Fe−OH	109.3°	109.3°
Fe−O−H	121.8°	121.8°
bond energy (Fe···OH_2)		
snap	16.43	22.30
adiabatic	12.87	12.86
(b) Cluster $Fe(OH)_3(H_2O)_2$ (OI)		
Fe···N	2.245 Å	2.245 Å
Fe···OH_2	2.317 Å	2.358 Å
Fe−OH	1.913 Å	1.930 Å
HO−Fe−OH	109.27°	105.97°
bond energy (Fe···OI)		
snap	23.67	36.96
adiabatic	16.56	16.57
(c) Fe_2O_3 Crystal		
	MS FF	exptl
Fe−O	1.946 Å	1.946 Å
Fe···O	2.087 Å	2.116 Å
O−Fe−O	102.1°	102.3°
Fe−O−Fe	119.2°	119.7°
O···Fe−O	162.2°	162.2°
lattice parameters		
$a = b$	5.00 Å	5.038 Å
c	13.76 Å	13.77 Å

TABLE 6: Snap Bond Energies (kcal/mol) for $Fe(OH)_3(OI)$ from *ab Initio* Quantum Mechanical Calculations

		snap bond energy	
method	basis set	OI-1-C	OI-1-H
UHF	LANL1DZ	69.7	68.5
UMP2	LANL1DZ	61.4	59.9
UHF	LAV3P**	64.0	63.3
UMP2	LAV3P**	58.4	57.6

carried out QM and MD studies. Three possible explanations come to mind:

1. modification in the binding of the OI to the iron oxide surface;

2. effect on the configuration of the hydrocarbon tail;

3. effect on the packing of H_2 O molecules in the cavity at the surface formed by the OI monolayer.

To consider the role of bond energy, we examined the snap binding energies of OI-1-C and OI-1-H (1-methylimidazoline) to $Fe(OH)_3$ using unrestricted Hartree−Fock (UHF) and second-order Møller−Plesset perturbative methods (UMP2) with the LANL1DZ[6,8] and LAV3P**[7,8] basis sets. These results (Table 6)[6,7] indicate that the deletion of a methyl group decreases the snap binding of the inhibitor by 1−2 kcal/mol out of 36 kcal/mol. This indicates that the large decrease in inhibition efficiency does not result from changes in the binding of the inhibitor to the surface.

A second function of the pendant group might be to restrict conformation of the hydrocarbon chain. Figure 5 shows the conformational energy (using the MS FF) as a function of N−C−C−C dihedral angle for three molecules:

a. OI-17(8═9)-CCN,

b. OI-17(8═9)-C, and

c. OI-17(8═9)-H. The energies were determined by keeping the hydrocarbon tail all-trans with the double bond in the cis position. The results indicate that a pendant group dramatically increases the steric energy of the molecule at 0° (overlap of carbon atoms) by 3 kcal/mol. This restriction of rotation about the C−C bond could be important in restricting the configuration involved in the monolayer. Free motion of the tail makes it easier for water to diffuse into a position on the surface between two different adsorbed tails. Attachment of the pendant group to an inhibitor molecule drastically restricts rotation of the hydrocarbon chain, leading to a barrier of 5.0 kcal for the methyl and aminoethyl side chains. Thus with the pendent group, an inhibitor molecule bound to a surface has its tail locked into position. This may lead to a rigid film, reducing free motion of water to the surface. This could be important for corrosion inhibition.

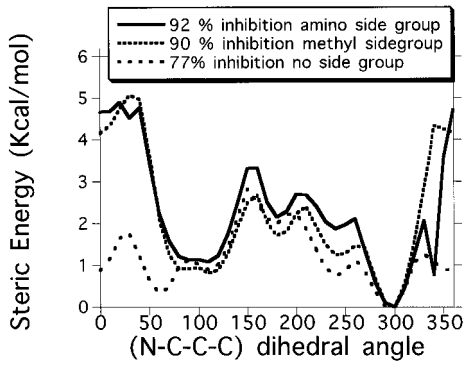

Figure 5. Steric energy vs N−C−C−C dihedral angle for 1-aminoethyl-2-oleicimidazoline (solid line, 92% CIE), 1-methyl-2-oleicimidazoline (dashed line, 90% CIE), and 2-oleicimidazoline (dotted line, 77% CIE).

Since the N−H bond is polar, such pendent groups may make DA bonds to additional Fe on the surface, dislodging additional H_2O. This may enhance stability. However, this may also encourage additional H_2O to remain in the cavity formed at the surface. This may be expelled at higher temperature, disordering the film.

3.0 Summary

We used quantum mechanical calculations on ferric clusters to i. develop the GVB model of crystalline α-Fe_2O_3, ii. determine the relative binding of OI and other nitrogen-containing molecules to $Fe(OH)_3(H_2O)_2$, iii. determine the relative binding of OI and H_2O to α-Fe_2O_3, iv. construct the MS FF for OI and α-Fe_2O_3, and v. assess the effect of the pendant group on configurational changes of the hydrocarbon tail. These results show that representative ferric clusters can be used to model the crystalline environment and to create an appropriate FF. This MS FF has now been used to study the mechanism of the corrosion inhibition of OI inhibitors.[17]

Acknowledgment. The research was funded by Chevron Petroleum Technology Company (thanks to R. Heming and F. McCaffery) and by DOE-BCTR (thanks to D. Boron). The facilities of the MSC are also supported by grants from NSF-GCAG (ASC 92-17368), NSF-CHE (95-22179), Aramco, Asahi Chemical, Owens-Corning, Chevron Chemical Company, Asahi Glass, Hercules, Avery Dennison, BP Chemical, Chevron Research and Technology Co., and Beckman Institute. Calculations for the project we carried out on the Pittsburgh, PA, San Diego, CA, and Illinois NSF Supercomputer Centers and on the JPL Cray.

References and Notes

(1) Edwards, A.; Osborne C.; Webster, S.; Klenerman, D.; Joseph, M.; Ostovar, P.; Doyle, M. *Corros. Sci.* **1994**, *36*, 315.

(2) Scully, J. C. *The Fundamentals of Corrosion*, 3rd ed.; Pergamon Press: Oxford, 1990.

(3) Uhlig, H. H.; Revie, R. W. *Corrosion and Corrosion Control*, 3rd ed.; Wiley: New York, 1985.

(4) Blake, R. L.; Hessevick, R. E.; Zoltai, T.; Finger, L. W. *Am. Mineral.* **1966**, *51*, 911.

(5) Hartree−Fock (HF) calculations using the 6-31G* basis set. The d^5 shell of Fe^{3+} is high spin ($S = {}^5/_2$) so that the UHF wave function was used.

(6) Frisch, M. J.; Trucks, G. W.; Head-Gordon M.; Gill, P. M. W.; Wong, M. W.; Foresman, J. B.; Johnson, B. G.; Schlegel, H. B.; Robb, M. A.; Replogle, E. S.; Gomperts, R.; Andres, J. L.; Raghavachari, K.; Binkley, J. S.; Gonzalez, C.; Martin, R. L.; Fox, D. J.; Defrees, D. J.; Baker, J.; Stewart, J. J. P.; Pople, J. A. *GAUSSIAN 92 Revision*; Gaussian Inc.: Pittsburgh, Pa, 1992.

(7) (a) Ringnalda, M. N.; Langlois J. M.; Greeley, B. H.; Murphy, R. B.; Russo, T. V.; Cortis C.; Muller R. P.; Marten, B.; Donnelly, R. E.; Mainz, D. T.; Wright J. R.; Pollard, T.; Cao, Y.; Won, Y.; Miller, G. H.; Goddard, W. A.; Freisner, R. A. *PS-GVB v2.2*; Schrodinger, Inc.: Portland, OR, 1995. (b) Greeley, B. H.; Russo, T. V.; Mainz, D. T.; Friesner, R. A.; Langlois, J.-M.; Goddard, W. A., III; Donnelly, R. E.; Ringnalda, M. N. *J. Chem. Phys.* **1994**, *101*, 4028.

(8) Hay, P. J.; Wadt, W. R. *J. Chem. Phys.* **1985**, *82*, 270; ibid, **1985**, *82*, 284.

(9) Hay, P. J.; Wadt, W. R. *J. Chem. Phys.* **1985**, *82*, 299.

(10) McLean, A. D.; Chandler, G. S. *J. Chem. Phys.* **1980**, *72*, 5639.

(11) Klenerman, D.; Hodge, J.; Joseph, M. *Corros. Sci.* **1994**, *36*, 301.

(12) Mayo, S. I.; Olafson, B. D.; Goddard, W. A., III. *J. Phys. Chem.* **1990**, *94*, 8897.

(13) Karasawa, N.; Dasgupta, S.; Goddard, W. A., III. *J. Phys. Chem.* **1991**, *95*, 2260.

(14) Rappé, A. K.; Goddard, W. A., III. *J. Phys. Chem.* **1991**, *95*, 3358.

(15) Ramachandran, S.; Lenz, T, G.; Skiff, W. M.; Rappé, A. K. *J. Phys. Chem.* **1996**, *100*, 5898.

(16) Stillinger, F. H.; Rahman, A. *J. Chem. Phys.* **1974**, *60*, 1545.

(17) Ramachandran, S.; Tsai, B.-L.; Blanco, M.; Chen, H.; Tang, Y.; Goddard, W. A., III. *Langmuir*, in press.